Tailoring *in vitro* evolution for protein affinity or stability

Lutz Jermutus*, Annemarie Honegger, Falk Schwesinger, Jozef Hanes†, and Andreas Plückthun‡

Biochemisches Institut, Universität Zürich, Winterthurerstrasse 190, CH-8057 Zürich, Switzerland

Edited by Gregory A. Petsko, Brandeis University, Waltham, MA, and approved October 16, 2000 (received for review July 5, 2000)

We describe a rapid and general technology working entirely *in vitro* to evolve either the affinity or the stability of ligand-binding proteins, depending on the chosen selection pressure. Tailored *in vitro* selection strategies based on ribosome display were combined with *in vitro* diversification by DNA shuffling to evolve either the off-rate or thermodynamic stability of single-chain Fv antibody fragments (scFvs). To demonstrate the potential of this method, we chose to optimize two proteins already possessing favorable properties. A scFv with an initial affinity of 1.1 nM (k_{off} at 4°C of 10^{-4} s^{-1}) was improved 30-fold by the use of off-rate selections over a period of several days. As a second example, a generic selection strategy for improved stability exploited the property of ribosome display that the conditions can be altered under which the folding of the displayed protein occurs. We used decreasing redox potentials in the selection step to select for molecules stable in the absence of disulfide bonds. They could be functionally expressed in the reducing cytoplasm, and, when allowed to form disulfides again, their stability had increased to 54 kJ/mol from an initial value of 24 kJ/mol. Sequencing revealed that the evolved mutant proteins had used different strategies of residue changes to adapt to the selection pressure. Therefore, by a combination of randomization and appropriate selection strategies, an *in vitro* evolution of protein properties in a predictable direction is possible.

Triggered by more facile structure determination and generally accessible homology modeling over the last decade, the deliberate change of biochemical or biophysical characteristics in proteins has relied mostly on hypothesis-based (''rational'') protein engineering. It has become increasingly apparent, however, that our present knowledge of structure–function relationships in proteins is still insufficient to make this a consistent and robust approach. The past few years have seen the emergence of directed protein evolution as an alternative experimental procedure that does not rely on precise structural information and prediction. In this approach, natural protein evolution, i.e., cycles of alternating diversification and subsequent selection or screening, is mimicked in the laboratory.

Directed protein evolution has been carried out previously by the use of selection technologies such as phage (e.g., 1–3), bacterial (4), or yeast display (5). Alternatively, mutant populations can be screened for improved variants by evaluating individual members and combining their mutations for the subsequent round (6). All of these approaches suffer from both the laborious alternation between *in vitro* diversification and *in vivo* selection or screening and the relatively small library size for each round of protein evolution. Screening is limited by the number of mutants that can be examined by automation, whereas selection is limited by the transformation step, and in selection systems usually larger numbers can be handled.

Ribosome display (reviewed in ref. 7) has previously been described as an alternative display method for both the selection (8–10) and evolution of ligand-binding proteins. It works by transcribing a library of DNA to mRNA, translating it *in vitro* with stoichiometric amounts of ribosomes such that at the end of the reaction, the protein (as peptidyl-tRNA), and the mRNA are still connected to the ribosome. This connection is achieved by the absence of a stop codon and a stabilizing buffer. Folding of the protein is allowed by its fusion to a C-terminal unstructured tether, which can occupy the ribosomal tunnel. In one report the "neutral" evolution of a single sequence without stringent selection (8) was described, and, in a subsequent study, a "built-in" affinity maturation was observed because of the natural error rate of *Taq* polymerase involved in the amplification and selection of single-chain Fv antibody fragments (scFvs) from libraries for antigen binding (11). One of the attractions of the method is that, because all steps are carried out *in vitro*, ribosome display selection can easily be combined with *in vitro* mutagenesis and recombination for cycles of protein evolution. The technology should be applicable to any protein for which a binding partner is available.

The present study demonstrates the potential of ribosome display for directed *in vitro* protein evolution. Combining this technology with DNA shuffling (12) and improved or novel selection strategies, we demonstrate that distinct and predictable biophysical characteristics of scFvs can be rapidly and efficiently evolved.

Experimental Protocol

Off-Rate Selection. *Library construction.* The library was PCR assembled in two steps from separate PCR fragments of the genes for the variable domains V_H, V_L, and the C-terminal spacer, and then the 5′ region was added by nested PCR of the whole construct (13). V_H and V_L of the scFv c12 (14) were amplified separately, by using primers SDA (13) with c12_linker (introducing a nonrepetitive linker between the two variable domains, 5′-CACCTCGGATCCMGRAGCAGAACYAGTNTBMGRAGCAGAACYACYNTBGCTCGCGCCGTTAGGACGTTTCAGCTC-3′) and c12_linkeradapt (5′-GGATCCGAGGTGCAGCTG-3′) with Sfi_rescue (5′-GCCCTCGGCCCCCGAGGC-3′), respectively. Here and in all further steps the resulting PCR products were separated on a 1.5% agarose gel and purified with the QIAquick gel extraction kit (Qiagen, Chatsworth, CA). Both fragments were assembled by PCR by using primers SDA and Sfi_rescue. In parallel, the spacer from gene3 of filamentous phage M13 was amplified from plasmid pAK200 (15) with primers Sfi_spacer (5′-GCCTCGGGGGCCGAGGGCGGCGGTT-3′) and geneIIItot (annealing at the 3′ end of the geneIII coding sequence, 5′-CTCCTTATTACGCAGTATGTTAGCAAACGTAGAAAATAC-3′). After gel purification, this spacer fragment and the scFv coding sequence were assembled by PCR, except that primers SDA and T3link (5′-CCAGTGAAGGTGAGCCTCAGTAGCGACAGAATCAA-3′) were added. For error-prone PCR, the fragment was amplified using standard conditions, except that 6-(2-deoxy-β-

This paper was submitted directly (Track II) to the PNAS office.

Abbreviation: scFvs, single-chain Fv antibody fragments.

*Present address: Cambridge Antibody Technology, The Science Park, Melbourn, Cambridgeshire SG8 6JJ, United Kingdom.

†Present address: Evotec Neurosciences GmbH, Schnackenburgallee 114, 22525 Hamburg, Germany.

‡To whom reprint requests should be addressed. E-mail: plueckthun@biocfebs.unizh.ch.

The publication costs of this article were defrayed in part by page charge payment. This article must therefore be hereby marked "*advertisement*" in accordance with 18 U.S.C. §1734 solely to indicate this fact.

Article published online before print: *Proc. Natl. Acad. Sci. USA*, 10.1073/pnas.011311398. Article and publication date are at www.pnas.org/cgi/doi/10.1073/pnas.011311398

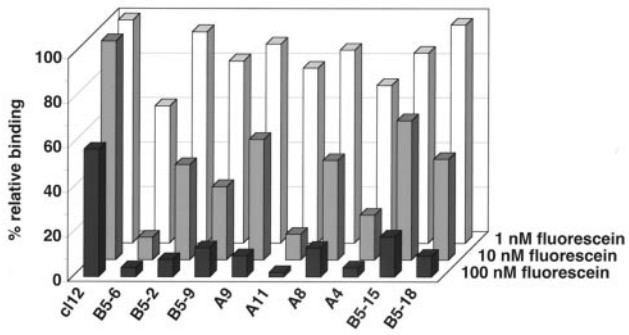

Fig. 1. Analysis of off-rate selections: semiquantitative inhibition RIA of selected c12 mutants (for details see *Experimental Protocol*). Kinetic and affinity parameters of purified c12 and three mutants were determined experimentally as described in the text. Because of the similar RIA profile of all mutants three c12 mutants of this set along with the parental protein were further analyzed. c12 wild-type: $k_{off} = 0.0028\,s^{-1}$, $k_{on} = 2.5 \times 10^6\,M^{-1}\,s^{-1}$, $K_{D,\,calc} = 1.1$ nM, $K_{D,\,titr} = 1.5$ nM; c12 B5–6: $k_{off} = 0.00014\,s^{-1}$, $k_{on} = 3.4 \times 10^6\,M^{-1}\,s^{-1}$, $K_{D,\,calc} = 0.04$ nM, $K_{D,titr} = 0.1$ nM; c12 B5–2: $k_{off} = 0.00020\,s^{-1}$; c12 B5–9: $k_{off} = 0.00018\,s^{-1}$. Measurements were performed at 25°C as described (19). $K_{D,\,calc}$ is the ratio obtained from the dissociation rate (k_{off}) and the association rate (k_{on}), and $K_{D,\,titr}$ is the equilibrium dissociation constant directly determined by titration. The error between duplicate measurements for k_{off} and k_{on} of all measured mutants is about ±3%; the error for $K_{D,\,titr}$ is about ±8%.

D-ribofuranosyl)-3,4-dihydro-8H-pyrimidino-[4,5-c][1,2]oxazin-7-one-triphosphate (dPTP) and 8-oxo-dGTP (Amersham Pharmacia; ref. 16) were added at 1/10 (20 μM) of the concentration of each dNTP (200 μM). The assembled band was gel purified and amplified with primers T7B and T3te (11). This PCR product was used directly for *in vitro* transcription as described (11).

Selection for improved off-rates. Ternary ribosomal complexes (mRNA-ribosome-scFv) displaying the library of antibody scFv fragment c12 were prepared by *in vitro* translation as described (13). Panning tubes (Nunc) blocked with 4% skimmed milk were prewashed with ice-cold PBS (10 mM sodium phosphate buffer, pH 7.4/140 mM NaCl/15 mM KCl) and washing buffer (50 mM Tris-acetate, pH 7.5/150 mM NaCl/50 mM $MgCl_2$/0.1% Tween 20). In these tubes, the centrifuged translation mixture was incubated with 1% sterilized and debiotinylated milk in the presence or absence (background control reaction) of 1 nM biotin-fluorescein (Sigma) and rotated within a larger ice-filled tube for at least 2 h. For off-rate selection, free fluorescein (Sigma) was added to 1 mM final concentration, and rotating on ice was continued for the indicated selection time. The translation mixture was added to the 10 μl of washed streptavidin magnetic beads and rotated on ice for 15 min. Beads were washed five times with 0.5 ml of washing buffer, and mRNA was eluted as described (13). mRNA purification, reverse transcription, and PCR were carried out according to published protocols (13). PCR primers were SDA and upA (annealing upstream of T3te on the geneIII coding sequence, 5′-CCTTATTAGCGTTTGCCATCTTTTCATAATCAAAATCACCGGAA-3′).

DNA shuffling. About 1 μg of gel-purified PCR products was incubated with DNase (Promega) as described (17). Fragments were separated on a 2% agarose gel, and DNA molecules smaller than 500 nt were excised and purified (QIAEX II; Qiagen). The assembly reaction was carried out with 45 cycles at an annealing temperature of 45° as described (17). The resulting PCR products were separated on a 1.5% agarose gel, and the band corresponding to the reassembled DNA was cut out and gel purified. This isolated band served as a template for the subsequent PCR with primers SDA and Sfi_rescue, which only amplified the scFv coding region.

RIA analysis of single mutants. After four rounds of directed *in vitro* evolution, the reverse transcription–PCR product was amplified with *Pfu* polymerase and primers SDA and Sfi_rescue to restore the restriction sites, and it was then cloned into the vector pTFT74 (18). Plasmid isolation, *in vitro* transcription, and translation in the presence of ^{35}S-labeled methionine (NEN) were carried out as described (13). The translation mixture was incubated with 0, 1, 10, and 100 nM fluorescein in 2% skimmed milk at 4°C for at least 2 h. These mixtures were briefly (10–15 min) incubated on microtiter plates coated with transferrin-fluorescein. Plates were washed five times with PBS with 0.05% Tween-20, and the remaining radioactivity was eluted with 0.1 M triethylamine and quantified by liquid scintillation counting.

Characterization of c12 mutants. Purification, determination of off- and on-rates, and K_D measurements by fluorescence titration were carried out as described (19). In brief, off-rates were measured in solution, using a competitive dissociation assay including a weakly fluorescent analog of fluorescein, 5-aminofluorescein (Sigma; ref. 20). Association kinetics were measured in solution with a stopped-flow fluorimeter (Hi-Tech Scientific, Salisbury, U.K.). The dissociation constants of fluorescein were determined at equilibrium by recording the fluorescence spectra from 505 to 525 nm, using a constant amount of fluorescein and variable scFv concentrations (21).

Stability Selection. *Library construction.* V_H and V_L of the anti-hag scFv (22) were amplified separately, using primers SDA (11) with hag_linker (introducing a nonrepetitive linker between the two variable domains, 5′-GAACTTCGGATCCMGRAGCAGAACYAGTNTBMGRAGCAGAACYACYNTBGCTCGCGCCGTTAGGAGCGCGCTTAAGT-3′) and hag_linkeradapt (5′-GGATCCGAAGTTCAACTA-3′) with *Eco*RI_rescue (5′-GTTGAGGGAATTCTCCGGAAGCTGA-3′), respectively. The two fragments were assembled as described above, except that primers SDA and *Eco*RI_rescue were added. In parallel, the spacer from gene3 of filamentous phage M13 was amplified with primers *Eco*RI_spacer (5′-TCAGCTTCCGGAGAATTCCCTCAA-3′) and geneIIItot. After gel purification this fragment and the spacer were assembled by PCR, further amplified, and transcribed *in vitro* as described above.

Selection under reducing conditions. In vitro translation for ribosome display selection was carried out as described (13), except that DTT was added during translation at the final concentration indicated. Translation reactions were stopped in washing buffer as described (13), which contained the same DTT concentration used during the *in vitro* translation. All other steps were carried out as described (13).

DNA shuffling. Shuffling was performed as described above, except that primer Sfi_rescue was replaced by primer *Eco*RI_rescue (see above).

RIA analysis of single mutants. After six rounds of directed *in vitro* evolution, single mutants were obtained as described above. Cell-free translation was carried out in duplicates for each RNA as outlined above, except that in one sample DTT was kept at a concentration of 10 mM during both *in vitro* translation and binding to transferrin-hag-peptide immobilized on microtiter plates.

Expression and purification of anti-hag mutants. Selected mutants were cloned into the expression vector pIG6 (23). The linker $(GGGGS)_6$ from plasmid pIG6 with the scFv anti-hag wild type was cloned between the two variable domains of the selected mutants. Proteins were expressed in *Escherichia coli* JM83 (24) and purified with a rapid two-column procedure coupling immobilized metal ion affinity chromatography (IMAC) and ion-exchange chromatography, using the BioCAD instrument (PerSeptive Biosystems, Framingham, MA) as described (23).

Urea equilibrium unfolding. scFv protein/denaturant mixtures (2 ml) containing a final protein concentration of 0.1 μM and urea concentrations varying from 0 to 7.5 M were prepared from purified scFv protein solution and urea stock solution (9 M) in Hepes-buffered saline as described previously (23). For equilibrium unfolding experiments with reduced protein the scFv

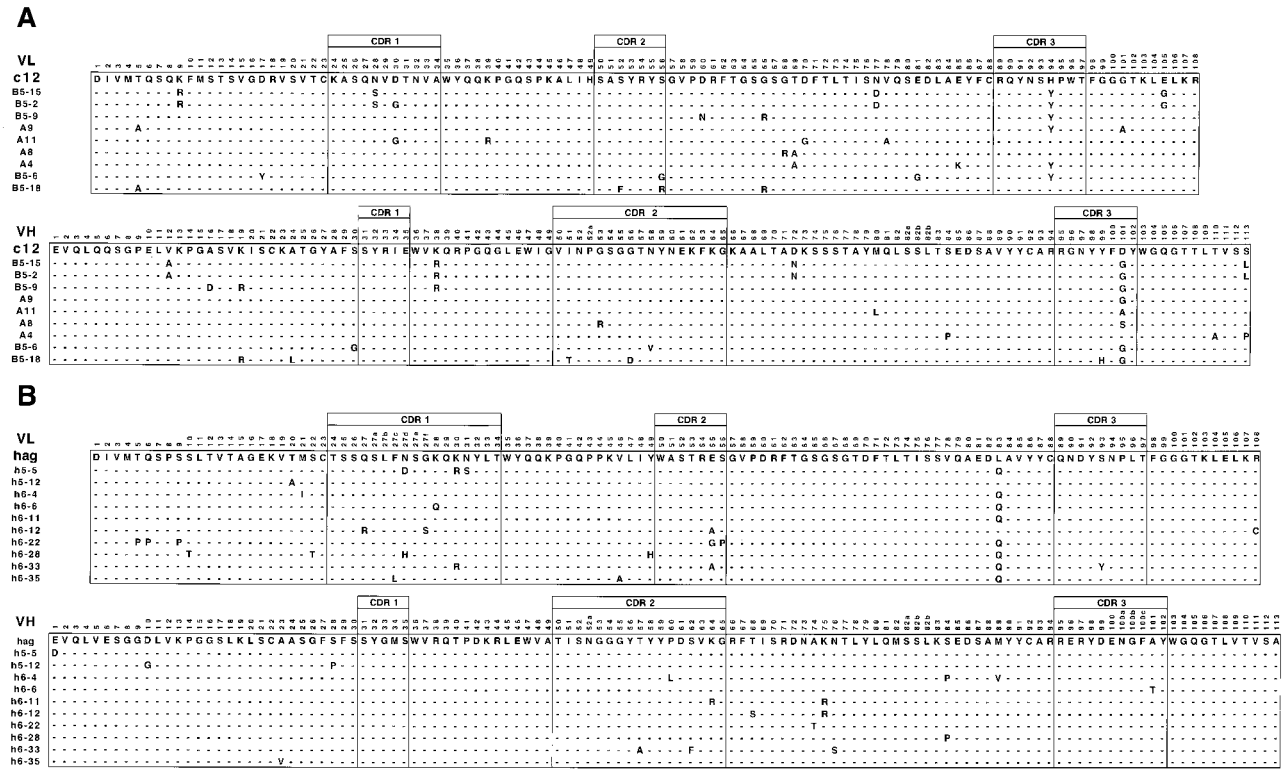

Fig. 2. Sequences of the selected clones. (*A* and *B*) Aligned sequences of affinity-matured c12 mutants (*A*) and of stability-matured hag mutants (*B*). Residue numbering and CDR localization are according to Kabat *et al.* (33).

fragment (0.75 μM) was incubated for several hours in 8 M urea and 20 mM DTT. The denatured and reduced protein was diluted in urea to give final concentrations from 0 to 4.5 M with a final DTT concentration of 10 mM and incubated at 20°C overnight. Fluorescence spectra were recorded as for the denaturation experiments. Data were evaluated using both two-state and three-state models (25), but because the three-state fit did not predict an additional stable species in the transition region, the results from the two-state model are reported.

Cytoplasmic expression and crude cell extract ELISA. ScFv anti-hag wild-type with either a 15-mer $(GGGGS)_3$ or 30-mer $(GGGGS)_6$ linker as well as selected mutants with their respective linkers from the selection were cloned into plasmid pTFT74 (18) and transformed into *E. coli* BL21 cells (26). Cells were grown at 25°C under the same conditions as for periplasmic expression, harvested after 3 h of induction, and resuspended in PBS with 10 mM DTT. The cell suspensions were lysed with a French press, and the crude cell extract was diluted 1:2 or 1:20 in PBS with a final concentration of 10 mM DTT and 2% skimmed milk. For testing inhibition with soluble antigen, hag-peptide was added to 1 μM concentration. Samples were allowed to bind to microtiter plates coated with transferrin-hag-peptide for 30 min at room temperature. Bound scFv protein was detected by using the monoclonal anti-myc-tag antibody 9E10 and a polyclonal anti-mouse/peroxidase conjugate (Pierce).

BIAcore kinetic measurements. A streptavidin-coated sensor chip SA (Amersham Pharmacia) was coated with biotinylated hag-peptide such that the maximal response was 150 RU to avoid rebinding. Kinetics of association and dissociation were monitored at a flow rate of 30 μl/min in Hepes-buffered saline buffer containing 0.005% Tween-20. Kinetics were measured at varying concentrations of scFv between 0.1 and 1 μM. The chip was regenerated with 0.1 M glycine·HCl (pH 2.2), and data were evaluated with a global fit in the BIAEVALUATION 3.0 software.

Results and Discussion

Affinity Evolution. *Selection for improved off-rates.* Preliminary experiments showed that in ribosome display the most efficient selection strategy for affinity maturation was off-rate selection. This approach has been used previously with phage (e.g., 2, 3) and yeast surface display (20). In ribosome display, selection has to occur at 4°C to maintain the stability of the ribosomal complexes. An initial library of the fluorescein-binding antibody c12 (14) with a starting K_D of 1.1 nM (see legend to Fig. 1) and an off-rate at 4°C in the range of 10^{-4} s^{-1} (19) was created by error-prone PCR (16). We first equilibrated ribosomal complexes coding for the protein library with nanomolar concentrations of biotinylated antigen and then added a large excess of free antigen. Time periods of off-rate selections were increased in each round (round 1, 2 h; round 2, 16 h; round 3, 48 h; round 4, 250 h) with DNA shuffling after each selection, and complexes still binding the biotinylated antigen were rescued by the addition of streptavidin-coated magnetic beads. The RNA coding for these proteins was purified and amplified by reverse transcription–PCR and, after DNA shuffling, served as a template for the next round of directed evolution. DNA smearing was avoided, even after over 100 PCR cycles per evolution round, by careful primer design such that the PCR product could be shortened in a stepwise manner during DNA shuffling (see *Experimental Protocol*). Despite the fact that RNA is generally considered a labile molecule, we could carry out the selection for a period of more than 10 days, provided that a high magnesium concentration and low temperature were maintained.

Affinity is improved 30-fold. After four rounds of DNA shuffling and off-rate selection, single mutants were analyzed after cell-free translation. To obtain a relative measure for affinity, binding of the *in vitro* produced protein to FITC coupled to Lys residues of BSA was determined after equilibration with low concentrations of soluble fluorescein. From the measurement of residual binding in the absence or presence of inhibitor we could estimate the relative

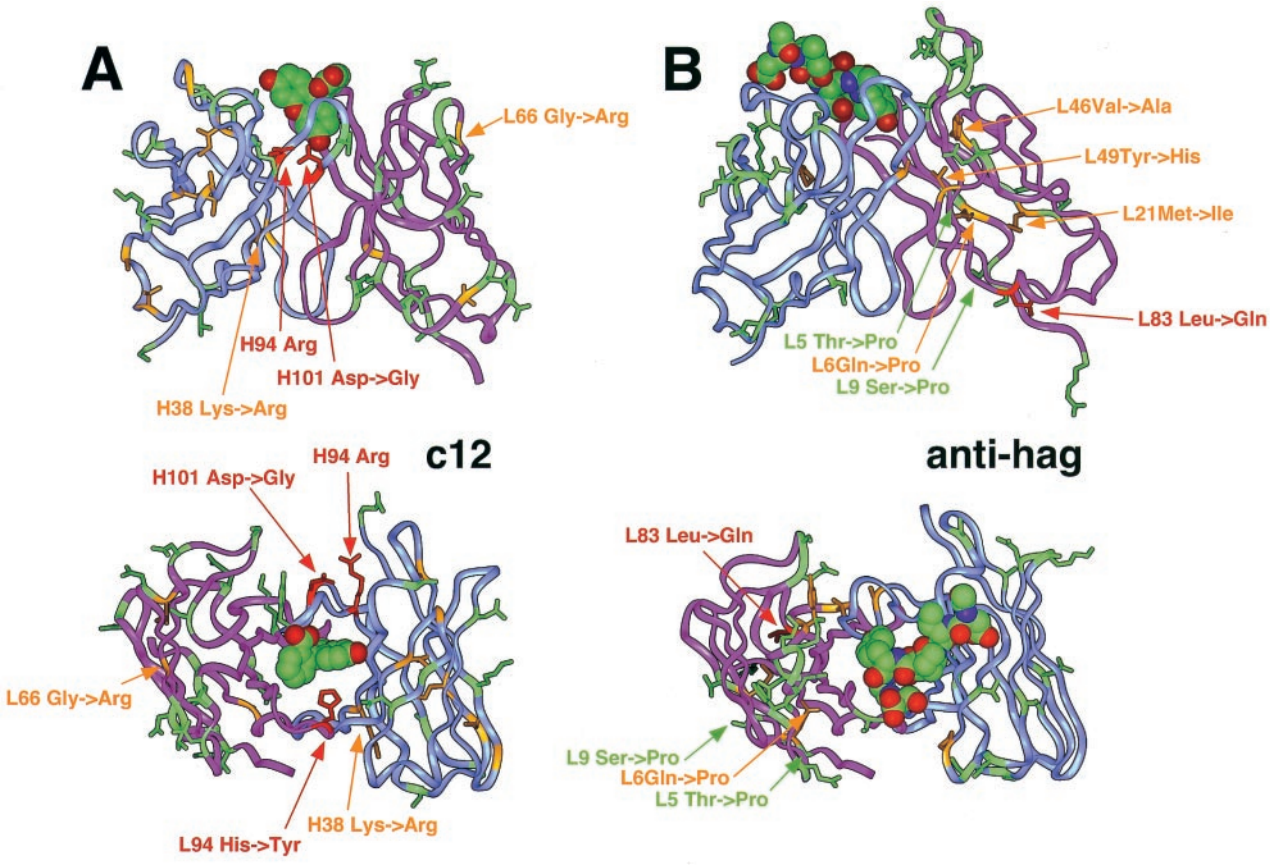

Fig. 3. Localization of the mutated residues in a three-dimensional model of c12 with docked fluorescein (theoretical model obtained by homology modeling, based on Protein Data Bank (PDB) entries 1iai, 1nca, 1igc for V_L; 1for, 1plg for V_H; and 1mim for CDR-H3) (*A*) and in the anti-influenza hemagglutinin antibody Fab 17/9 [experimental structure, PDB entry 1ifh (34)] (*B*). V_H is shown in blue; V_L is in purple. The strongly selected mutations anti-hag L83 Leu to Gln, c12 L94 His to Tyr, and c12 H101 Asp to Gly, Ser, or Ala and its salt-bridge partner Arg H94 are indicated in red. The positions of the remaining mutated residues are indicated by orange if the affected side chains are buried in the domain core and by green if they are located on the surface of the molecule.

differences between mutant proteins and their wild type (Fig. 1). SDS/PAGE analysis confirmed that similar protein amounts for all mutants were synthesized *in vitro* (data not shown). Three selected mutants were expressed in the *E. coli* periplasm as described in the experimental protocol. Measurements of k_{on}, k_{off}, and K_D (legend to Fig. 1) showed that k_{off} and, as a consequence, K_D had been improved by more than one order of magnitude. In addition, we concluded that the semiquantitative RIA described above is a valuable and rapid tool for assessing the relative binding affinity of *in vitro* produced protein.

With the exception of two positions, the selected amino acid changes are scattered over the sequence. Six additional mutants with improved signals in the prescreening were sequenced (Fig. 2*A*). The evolved scFvs all contained multiple mutations, compared with the parent molecule (4–11 amino acids, mean value of 7.2 per scFv). Many mutations were found only once or twice, and they probably represent "neutral" mutations accumulated during the randomization process. Only two positions are mutated in the majority of all sequences, indicating a strong selection: the mutation of His L94 to tyrosine in complementarity determining region L3 (CDR L3) affects a residue that points straight into the antigen binding site (Fig. 3*A*). Although the exact binding mode of the hapten to the c12 scFv has not yet been determined experimentally, a direct interaction of this mutated residue with the antigen is very likely.

The mutation of Asp H101 to glycine, alanine, or serine in CDR H3 affects a residue on the outer side of CDR H3, pointing away from the antigen-binding pocket. However, in a majority of all antibody structures, Asp H101 forms a salt bridge with Arg H94 (27). Substitution of Asp H101 by any small, noncharged residue will have the effect of breaking the salt bridge and increasing the flexibility of CDR H3. In antibodies containing the salt bridge, the CDR H3 can be seen to frequently twist and bend to obstruct the hapten-binding pocket, whereas antibodies lacking this feature often show a more "open" conformation. Because Asp H101 was replaced by glycine, serine, and alanine, each requiring different nucleotide substitutions, this removal of the salt bridge has occurred several times independently during the *in vitro* evolution, suggesting a strong selection.

Stability Evolution. *Selection by in vitro translation under reducing conditions.* scFvs contain two conserved disulfide bridges, one in each variable domain. These are important stability elements, and the removal of the disulfide bond results in a significant or even total loss of activity (e.g., 28, 29). We used this observation to define a strategy for selecting for improved stability. As we had shown previously that oxidizing conditions during *in vitro* translation are necessary for maximal yields of functional scFv protein (28), we selected for more stable mutants by choosing a reducing redox potential during the translation step in ribosome display. Over five rounds the selection pressure was gradually increased from 0.5 mM to 10 mM DTT (round 1, 0.5 mM DTT; round 2, 2 mM; round 3, 4 mM; round 4, 8 mM; round 5, 10 mM; with DNA shuffling after each selection). Mutants could survive the selection process only if they folded stably in the presence of DTT and retained their antigen-binding activity. Similar strategies, without the capacity to

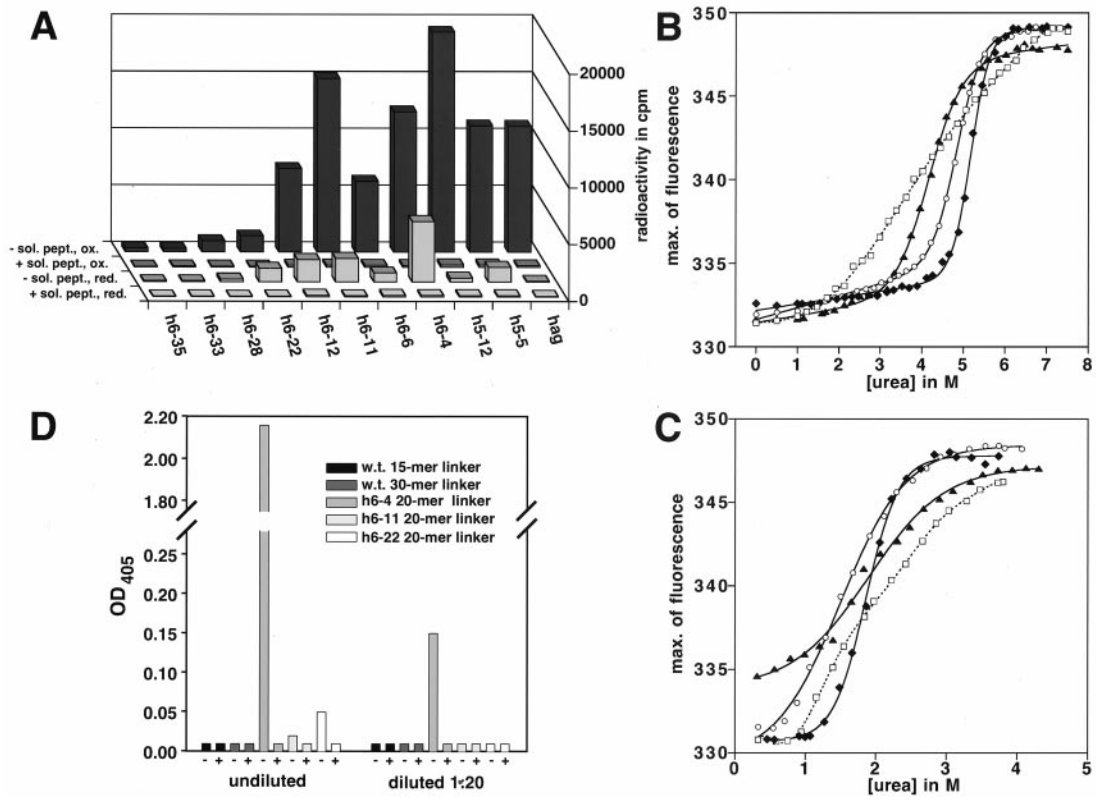

Fig. 4. Analysis of stability-matured hag mutants after *in vivo* and *in vitro* expression. Absolute RIA signal after reducing and oxidizing *in vitro* translation (*A*) and demonstration of specific binding by inhibition with 1 μM soluble hag peptide signals from *in vitro* translation under oxidizing conditions (*ox*) or reducing conditions (*red*) are shown. + or −*sol. peptide* indicates the presence or absence of 1 μM hag peptide as a competitor. By subtraction of the radioactivity of samples that were inhibited from the radioactivity of the uninhibited samples, the inhibitable portion of the RIA signal was obtained as a measure for specific binding activity. The resulting ratios of relative binding are calculated by dividing the inhibitable portion of the RIA signal in the presence of 10 mM DTT by the inhibitable RIA signal in the absence of DTT. They are as follows: anti-hag scFv wild-type: 0.2%; h5–5: 10.9%; h5–12: 1.6%; h6–4: 40.8%; h6–6: 11.1%; h6–11: 13.1%; h6–12: 26.4%; h6–22: 84.5%; h6–28: 20.9%; h6–33: 17.9%; h6–35: 17.0%. Urea denaturation at 10°C (*B*) of periplasmically produced hag wild-type and mutant proteins. ▲, Anti-hag wild-type scFv; ○, mutant h6–11; □, mutant h6–4; ◆, mutant h6–22. (*C*) Urea equilibrium renaturation under reducing conditions at 20°C of periplasmically produced hag wild-type and mutant proteins. (*D*) Normalized crude cell lysate ELISA after expression of hag wild-type and mutant proteins at 25°C in the cytoplasm of *E. coli*. Bars represent the binding signals of active protein in the absence (−) and presence (+) of competing soluble hag-peptide (1 μM), to indicate specific binding.

gradually increase selection pressure, however, have been described previously for the *in vivo* selection of improved stability (29, 30). The oxidized form of the model protein in this directed evolution experiment, anti-hag scFv (22), had a midpoint of denaturation of 4.5 M urea and, under the assumption of two-state unfolding, a stability of 24 kJ/mol. Both of these values are typical for antibody scFv fragments.

Many mutants with different sequence changes are able to fold in a reducing in vitro translation system. The sequence pool was assayed by *in vitro* translation after each round. An antigen-specific signal after translation under reducing conditions could be detected after four cycles of directed evolution. Single clones after five rounds were analyzed by *in vitro* translation under both oxidizing and reducing conditions (Fig. 4*A*). By relating the amount of functional protein produced in these two experiments (see legend to Fig. 4), we had a direct measure of the relative stability of the mutants, independent of their respective affinities, which may also influence the total RIA signal (Fig. 4*A*). SDS/PAGE and subsequent autoradiography (data not shown) showed that wild-type and mutant proteins were equally reduced upon cell-free production in the presence of DTT and that the same amount of protein was produced in both the absence and presence of DTT. The binding differences observed in the RIA experiment were therefore due exclusively to folding. From 48 evolved clones tested, about 65% showed functionality when they were expressed in the presence of 10 mM DTT (i.e., more than 2% relative binding).

With one exception, the selected amino acid changes are scattered over the sequence. Ten mutants were sequenced (Fig. 2*B*). As seen in the affinity evolution (see above), the sequences for these clones were very different (three to seven mutations, mean value of 4.8 per scFv). In 80% of the clones sequenced, the semiexposed leucine residue in position L83 has been replaced by a glutamine (Fig. 3*B*). A similar replacement of Leu L83 by an alanine residue had been found to have a positive effect on protein production in a fusion of a Fab fragment with a superantigen (31). There is no other position in the anti-hag sequence that shows such a clear selection of a mutation as L83. However, it is striking how strongly mutations in buried and semiburied positions are concentrated in the V_L domain (Met L21 Ile, Val L46 Ala, Tyr L49 His), whereas the V_H domain predominantly accumulated surface and interface mutations (Fig. 3*B*). This difference in the two domains suggests that in this scFv fragment the stability of the V_L domain is limiting the overall stability of the heterodimer, an interpretation substantiated by earlier measurements (23).

Selected mutants are chemically more stable than the wild-type protein. We chose three mutants, h6–4, -11, and -22, for further analysis. Wild-type and mutant proteins with the identical interdomain linker $(GGGGS)_6$ were expressed in the periplasm of *E. coli* JM83 (24) as described. Surprisingly, all mutants gave higher yields (up to 4-fold) of functional protein than the wild-type protein. Gel filtration analysis, also after several days of storage, demonstrated that all four proteins were monomers without unpaired cysteine residues (data not shown).

BIOCHEMISTRY

Urea denaturation experiments of the purified mutants showed a clear shift of the transition midpoint to higher denaturant concentrations, compared with the purified wild-type protein (Fig. 4*B*). The most stable protein was mutant h6–22 with a $\Delta\Delta G$ of 30 kJ/mol and a shift of the denaturation midpoint by 0.9 M urea. This protein followed a two-state mechanism, as its *m*-value (10.4 kJ mol^{-1} M^{-1}), i.e., the "steepness" of the fit in Fig. 4*B*, was close to the theoretical number (32) of 10.9 kJ mol^{-1} M^{-1}. It has to be noted, however, that the wild-type protein and mutant h6–11 give *m* values of 5.8 and 7.9 kJ mol^{-1} M^{-1} and thus may not follow true two-state transitions, so that their ΔG values have to be treated with some caution.

Because selection was carried out under reducing conditions we also tested the stabilities of the four proteins in their reduced form (Fig. 4*C*). All mutants reattained the native state after refolding from the denatured and reduced state. In contrast, the wild-type protein did not fully reach the fluorescence maximum of the native state, indicating a population of nonnative species remaining after refolding and, thus, incomplete reversibility. The ranking from the RIA experiments (see relative binding percentages in legend to Fig. 4) was confirmed by the equilibrium unfolding experiments under both reducing and nonreducing conditions (Fig. 4 *B* and *C*).

The selected mutants can be functionally expressed in the cytoplasm. The three selected mutants and the wild-type protein with two different linkers, $(GGGGS)_3$ and $(GGGGS)_6$, were expressed in the cytoplasm of *E. coli* BL21 (26) as described, and the normalized crude cell extract was used for ELISA (Fig. 4*D*). In this case, it was not the most stable protein of the analyzed mutant set that showed the highest signal, but mutant h6–4. The reason for this result might be better *in vivo* expression and/or folding yield at the growth temperature.

The result of the ELISA with crude cytoplasmic extracts correlates well with the absolute RIA signals after reducing *in vitro* translation (Fig. 4*A*). Because the S30 *E. coli* cell extract is a cytoplasmic extract, *in vitro* translation under reducing conditions seems to mimic the *in vivo* conditions rather well and can therefore be used to rapidly assess the potential performance of normally disulfide-containing proteins in the reducing cytoplasm. The signal differences were not due to improved binding, as the association and dissociation rates determined by BIAcore kinetic measurements did not change within the experimental error (data not shown).

Conclusions

A generic approach to directed evolution, occurring totally *in vitro*, is described that can be tailored toward either affinity or stability. Because ribosome display selections do not require any transformation steps, the presented process is very fast, and up to five rounds of evolution can be accomplished within 2 weeks. Furthermore, it is compatible with all methods of *in vitro* mutagenesis. Protein optimization by ribosome display does not depend on details of a structural model or predictions; nor is it necessary to limit the initial library to a small randomized sequence stretch (such as the CDR regions). This study rather shows that improved protein variants can be selected and evolved by using random mutagenesis over the entire sequence. Both experiments resulted in several mutants with improved characteristics making up a majority of the sequence pool after directed *in vitro* evolution. As a consequence, the screening of 48 protein variants after each maturation experiment gave more than 50% of improved mutants.

Because the ribosomal complexes are stable for long time periods at 4°C, it is possible to select for very slow off-rates at that temperature. Whereas the relative ranking of mutants hardly changes with temperature (19), these off-rates can increase by more than one order of magnitude when measured under physiological conditions (above 20°C). Further improvements of ribosome display technology should therefore concentrate on the stabilization of the ternary ribosomal complex of mRNA, ribosome, and displayed protein to allow selections at higher temperatures for equally long time periods.

Furthermore, directed evolution with ribosome display selects from large populations in each cycle such that several mutant lineages can be followed simultaneously. For example, the mutation of Asp H101 to a smaller residue occurred several times independently as the selected Gly, Ser, and Ala mutations each required different base pair changes. This observation of independent lineages becomes even more evident in the stability selection. Here, sequencing revealed that, except for a single more frequent amino acid exchange, all analyzed clones had acquired different additional mutations to adapt to the selection pressure.

In summary, we have shown that starting from scFv molecules with typical or even favorable values for affinity or stability, a directed *in vitro* evolution approach with ribosome display is able to further improve these proteins. For this purpose, we optimized or established novel selection strategies and provide two examples of protein evolution tailored for the physical property desired, carried out totally *in vitro*. We have also demonstrated that simple assays based on *in vitro* translation can be used to rapidly estimate both the stability and affinity of disulfide-containing ligand-binding proteins.

We thank Kathrin Ramm and Alain Tissot for technical advice and discussions. We are indebted to Stephen Marino for critical reading of the manuscript and helpful suggestions. L.J. was supported by a predoctoral Kekulé Fellowship from the Fonds der Chemischen Industrie (Frankfurt, Germany).

1. Roberts, B. L., Markland, W., Ley, A. C., Kent, R. B., White, D. W., Guterman, S. K. & Ladner, R. C. (1992) *Proc. Natl. Acad. Sci. USA* **89,** 2429–2433.
2. Hawkins, R. E., Russell, S. J. & Winter, G. (1992) *J. Mol. Biol.* **226,** 889–896.
3. Chen, Y., Wiesmann, C., Fuh, G., Li, B., Christinger, H. W., McKay, P., de Vos, A. M. & Lowman, H. B. (1999) *J. Mol. Biol.* **293,** 865–881.
4. Daugherty, P. S., Chen, G., Iverson, B. L. & Georgiou, G. (2000) *Proc. Natl. Acad. Sci. USA* **97,** 2029–2034. (First Published February 25, 2000; 10.1073/pnas.030527597)
5. Holler, P. D., Holman, P. O., Shusta, E. V., O'Herrin, S., Wittrup, K. D. & Kranz, D. M. (2000) *Proc. Natl. Acad. Sci. USA* **97,** 5387–5392. (First Published April 25, 2000; 10.1073/pnas.080078297)
6. Schmidt-Dannert, C. & Arnold, F. H. (1999) *Trends Biotechnol.* **17,** 135–136.
7. Jermutus, L., Ryabova, L. A. & Plückthun, A. (1998) *Curr. Opin. Biotechnol.* **9,** 534–548.
8. Hanes, J. & Plückthun, A. (1997) *Proc. Natl. Acad. Sci. USA* **94,** 4937–4942.
9. He, M. & Taussig, M. J. (1997) *Nucleic Acids Res.* **25,** 5132–5134.
10. He, M., Menges, M., Groves, M. A., Corps, E., Liu, H. Brüggemann, M. & Taussig, M. J. (1999) *J. Immunol. Methods* **231,** 105–17.
11. Hanes, J., Jermutus, L., Weber-Bornhauser, S., Bosshard, H. R. & Plückthun, A. (1998) *Proc. Natl. Acad. Sci. USA* **95,** 14130–14135.
12. Stemmer, W. P. (1994) *Proc. Natl. Acad. Sci. USA* **91,** 10747–10751.
13. Hanes, J., Jermutus, L. & Plückthun, A. (2000) *Methods Enzymol.* **328,** 404–430.
14. Hanes, J., Jermutus, L., Schaffitzel, C. & Plückthun, A. (1999) *FEBS Lett.* **450,** 105–115.
15. Krebber, A., Bornhauser, S., Burmester, J., Honegger, A., Willuda, J., Bosshard, H. R. & Plückthun, A. (1997) *J. Immunol. Methods* **201,** 35–55.
16. Zaccolo, M., Williams, D. M., Brown, D. M. & Gherardi, E. (1996) *J. Mol. Biol.* **255,** 589–603.
17. Adey, N. B., Stemmer, W. P. C. & Kay, B. K. (1996) in *Phage Display of Peptides and Proteins. A Laboratory Manual*, eds. Kay, B. K., Winter, J. & McCafferty, J. (Academic, London), pp. 280–292.
18. Ge, L., Knappik, A., Pack, P., Freund, C. & Plückthun, A. (1995) in *Antibody Engineering*, ed. Borrebaek, C. A. K. (Oxford Univ. Press, New York), pp. 229–266.
19. Schwesinger, F., Ros, R., Strunz, T., Anselmetti, D., Güntherodt, H. J., Honegger, A., Jermutus, L., Tiefenauer, L. & Plückthun, A. (2000) *Proc. Natl. Acad. Sci. USA* **97,** 9972–9977.
20. Boder, E. T. & Wittrup, K. D. (1997) *Nat. Biotechnol.* **15,** 553–557.
21. Pedrazzi, G., Schwesinger, F., Honegger, A., Krebber, C. & Plückthun, A. (1997) *FEBS Lett.* **415,** 289–293.
22. Krebber, C., Spada, S., Desplancq, D. & Plückthun, A. (1995) *FEBS Lett.* **377,** 227–231.
23. Spada, S., Honegger, A. & Plückthun, A. (1998) *J. Mol. Biol.* **283,** 395–407.
24. Yanisch-Perron, C., Vieira, J. & Messing, J. (1985) *Gene* **33,** 103–119.
25. Pace, C. N. (1990) *Trends Biotechnol.* **8,** 93–98.
26. Studier, F. W. & Moffatt, B. A. (1986) *J. Mol. Biol.* **189,** 113–130.
27. Morea, V., Tramontano, A., Rustici, M., Chothia, C. & Lesk, A. M. (1998) *J. Mol. Biol.* **275,** 269–294.
28. Ryabova, L. A., Desplancq, D., Spirin, A. S. & Plückthun, A. (1997) *Nat. Biotechnol.* **15,** 79–84.
29. Proba, K., Wörn, A., Honegger, A. & Plückthun, A. (1998) *J. Mol. Biol.* **275,** 245–253.
30. Martineau, P., Jones, P. & Winter, G. (1998) *J. Mol. Biol.* **280,** 117–127.
31. Forsberg, G., Forsgren, M., Jaki, M., Norin, M., Sterky, C., Enhorning, A., Larsson, K., Ericsson, M. & Bjork, P. (1997) *J. Biol. Chem.* **272,** 12430–12436.
32. Myers, J. K., Pace, C. N. & Scholtz, J. M. (1995) *Protein Sci.* **4,** 2138–2148.
33. Kabat, E. A., Wu, T. T., Perry, H. M., Gottesmann, K. S. & Foeller, C. (1991) *Sequences of Proteins of Immunological Interest* (National Institutes of Health, Bethesda, MD).
34. Schulze-Gahmen, U., Rini, J. M. & Wilson, I. A. (1993) *J. Mol. Biol.* **234,** 1098–1118.